Supporting Information for

Monometallic lanthanide salicylhydrazone complexes exhibiting strong near-infrared luminescence

Kaitlynn M. Ayers, Nathan D. Schley, Gaël Ung*

Department of Chemistry, University of Connecticut, 55 N. Eagleville Road, U-3060, Storrs, CT, 06269-3060, USA

E-mail: gael.ung@uconn.edu

Contents

Experimental Section

Chemicals and Reagents……S2
Apparatus……S2 – S3
Synthesis of Na_2ONO (L^{2-})……S3
Syntheses of Ln tetrakis(pyridylmethyl)ethylenediaminetris(triflate)……S3 – S4
Syntheses of [Ln(ONO)tpen](OTf) complexes……S4 – S6

NMR

Na_2ONO (L^{2-})……^{1}H: S6
[Nd(tpen)$(OTf)_3$)] complex……^{1}H: S7
^{19}F: S7
[Er(tpen)$(OTf)_3$)] complex……^{1}H: S8
[Yb(tpen)$(OTf)_3$)] complex……^{1}H: S8
^{19}F: S9
[Nd(ONO)tpen](OTf) complex……^{1}H: S9
^{19}F: S10
[Er(ONO)tpen](OTf) complex…… ^{1}H: S10
^{19}F: S11
[Yb(ONO)tpen](OTf) complex…… ^{1}H: S11
^{19}F: S12
[Nd(ONO)tpen](OTf) variable temperature ^{1}H……S12

High Resolution Mass Spectrometry

[Nd(ONO)tpen](OTf) complex……S13
[Er(ONO)tpen](OTf) complex……S13
[Yb(ONO)tpen](OTf) complex……S14

Photophysical Data

Absorption and emission of LH_2 ligand……S14
Excitation, emission, and absorption of [Nd(ONO)tpen](OTf)…… S15
Excitation, emission, and absorption of [Yb(ONO)tpen](OTf)…… S15
[Yb(ONO)tpen](OTf) emission in water:ACN……S16
Quantum Yield Determination……S16 –S17

X-Ray Crystallography Data

N_{tpen} – Ln bond distances……S18
Geometry comparison of precursors and products……S18
[Nd(ONO)tpen](OTf) complex……S19
[Er(ONO)tpen](OTf) complex……S20
[Yb(ONO)tpen](OTf) complex……S21

Experimental Section

Chemicals and Reagents

Hydrazine monohydrate ($H_2NNH_2 \cdot H_2O$, 99+%), salicylaldehyde ($C_7H_6O_2$, 99%), calcium hydride (CaH, ≥2mm anh; 90-95%), ethylenediamine ($C_2H_8N_2$, 99%), neodymium trifluoromethanesulfonate ($Nd(OSO_2CF_3)_3$, 98%), and sodium hydride (NaH, in mineral oil; 57-63%) were purchased from Alfa Aesar. Erbium trifluoromethanesulfonate ($Er(OSO_2CF_3)_3$), ytterbium trifluoromethanesulfonate ($Yb(OSO_2CF_3)_3$), and 2-chloromethylpyridine hydrochloride ($C_6H_6ClN \cdot HCl$) were purchased from Oakwood Chemical. Cetyltrimethylammonium chloride ($CH_3(CH_2)_{15}N(Cl)(CH_3)_3$, 25wt% solution) was purchased from Sigma Aldrich and methyl 4-tert-butylbenzoate ($(CH_3)_3CC_6H_4CO_2CH_3$, >98%) was purchased from TCI Chemicals. Sodium hydride was rinsed several times with pentane to remove the mineral oil residue on a medium porosity glass frit and then dried under vacuum. All other reagents were used without further purification. Tetrakis(pyridylmethyl)ethylenediamine (tpen) and the 4-tert-butylsalicylhydrazone ligand (LH_2) were prepared according to literature.[1,2] Any solvents used were dried using a solvent purification system from Pure Process Technologies or distilled under nitrogen atmosphere after stirring overnight over CaH. All metal reaction manipulations were carried out in a Vigor glove box filled with a nitrogen atmosphere.

Apparatus

All NMR spectra were obtained using a Bruker AVANCE 300 MHz or Bruker AVANCE III 400 MHz Spectrometer. Chemical shifts are reported in parts per million relative to the residual solvent peak in each deuterated solvent for ^1H and relative to $BF_3(C_4H_{10}O)$ for ^{19}F. Absorption and excitation spectra were collected on a HORIBA Duetta Spectrophotometer using HORIBA EzSpec software. Emission spectra were conducted on an Edinburgh FLS1000 Spectrophotometer equipped with PMT 980 and InGaAs detectors and a temperature control sample chamber using Fluoracle software. Absolute quantum yields were determined using the Edinburg spectrophotometer equipped with a barium sulfate coated integration sphere. Quantum yield were determined using a reference peak from the visible range to scale the remainder of the emission spectrum from the alternate detector and determine the overall

quantum yield. High resolution mass spectrometry was done for all complexes using an Applied Biosystems Sciex Qstar Elite LC Mass Spectrometer located in the University of Connecticut Mass Spectrometry Lab. Single-crystal X-ray diffraction studies were performed at Vanderbilt University: a suitable crystal of each sample was selected for analysis and mounted in a polyimide loop. All measurements were made on a Rigaku Oxford Diffraction Supernova Eos CCD with filtered Cu Kα or Mo Kα radiation at a temperature of 100 K. Using Olex2,[3] the structure was solved with the ShelXT structure solution program using direct methods and refined with the ShelXL refinement package[4] using least squares minimization.

Synthesis of Na_2ONO (L^{2-})

To a 20 mL scintillation vial 50 mg (0.1701 mmol, 1 eq) of the salicylhydrazone ligand was added with about 4 mL of THF and a stir bar. Next 10 mg (0.4167 mmol, 2.45eq) NaH was added to the stirring solution for an immediate color change from clear to neon yellow green and the creation of hydrogen gas bubbles. The solution was stirred until no more bubbles emerged from the solution, it was then filtered through a pipet with a plug of celite and a filter paper to remove any excess NaH. The pipet was rinsed through with clean THF to collect as much of the ligand as possible and the solvent was removed in vacuo to afford 49 mg (85%) of the Na_2ONO complex as a bright yellow green solid. ^{1}H NMR (CD_3CN, 400 MHz): δ (ppm) 1.30 (s, 9H, -C(C**H**$_3$)$_3$), 6.25 (m, 1H, C**H**$_{AR}$), 6.45 (m, 1H, C**H**$_{AR}$), 6.84, (s (br), 1H, C**H**$_{AR}$), 7.03 (d, *J = 7.16*, 1H, C**H**$_{AR}$), 7.25 (s (br), 2H, C**H**$_{AR}$), 8.00 (d, *J = 1.72*, 2H, C**H**$_{AR}$), 8.35 (s, 1H, -NC**H**-).

Synthesis of neodymium tetrakis(pyridylmethyl)ethylenediaminetris(triflate) [Nd(tpen)(OTf)$_3$]

The synthesis for the neodymium tpen salt [Nd(tpen)(OTf)$_3$] was adapted from Natrajan et al.[5] To a 20 mL scintillation vial, tpen (100 mg, 0.2355 mmol) was added with 6 mL of acetonitrile (ACN). Next, neodymium(III) trifluoromethanesulfonate was weighed in a 4 mL vial (139 mg, 0.2350 mmol) and the solid was carefully added into the stirring ligand solution. The reaction mixture goes from cloudy and opaque to clear. Using a pipet, some of the reaction solution was used to rinse the 4 mL vial twice to ensure all solid was added to the reaction. The reaction was stirred for two hours to ensure all solid entered solution for a complete reaction. Then solvent was removed in vacuo to yield 203 mg of the desired product as a light amber

solid (85% yield). ^{1}H NMR (CD_3CN, 400 MHz): δ (ppm) 3.46 (m), 3.68, 6.96, 8.95, 12.08. The NMR is broad due to fluxionality of ligand in solution showing the average of the species with differing ligand positions. As a result, accurate integrations for the spectra cannot be provided. All efforts to obtain ^{13}C NMR were unsuccessful due to paramagnetism in the compound. ^{19}F NMR (CD_3CN, 376.512 MHz): δ (ppm) 78.89 (s, 9F, $^{-}OSO_2C\mathbf{F_3}$). HRMS calculated for $C_{28}H_{28}N_6F_6NdO_6S_2^+$ ([M - ($^{-}OSO_2CF_3$)]$^+$): calculated 864.0488, found 864.0231.

Synthesis of erbium tetrakis(pyridylmethyl)ethylenediaminetris(triflate) [Er(tpen)(OTf)$_3$]

The same procedure as above was followed in the preparation of the erbium salt [Er(tpen)(OTf)$_3$]. ^{1}H NMR (CD_3CN, 400 MHz): δ (ppm) -93.49, -71.80, -10.33, -5.68, 3.32, 4.12, 7.23, 7.62, 8.46, 14.98, 18.08, 27.38, 32.02, 36.37, 100.72. The NMR is broad due to fluxionality of ligand in solution showing the average of the species with differing ligand positions. As a result, accurate integrations for the spectra cannot be provided. All efforts to obtain ^{13}C NMR were unsuccessful due to paramagnetism in the compound. ^{19}F NMR: due to paramagnetism the peak is broadened into the baseline and is difficult to determine. HRMS calculated for $C_{28}H_{28}N_6F_6ErO_6S_2^+$ ([M - ($^{-}OSO_2CF_3$)]$^+$): calculated 888.0713, found 888.0678.

Synthesis of ytterbium tetrakis(pyridylmethyl)ethylenediaminetris(triflate) [Yb(tpen)(OTf)$_3$]

The same procedure as above was followed in the preparation of the ytterbium salt [Yb(tpen)(OTf)$_3$]. ^{1}H NMR (CD_3CN, 400 MHz): δ (ppm) -44.05, -35.76, -28.60, -25.19, -16.15, -2.54, 3.40, 4.19, 7.29, 7.69, 8.51, 9.95, 18.99, 20.55, 25.31, 47.15. The NMR is broad due to fluxionality of ligand in solution showing the average of the species with differing ligand positions. As a result, accurate integrations for the spectra cannot be provided. All efforts to obtain ^{13}C NMR were unsuccessful due to paramagnetism in the compound. ^{19}F NMR (CD_3CN, 376.512 MHz): δ (ppm) -78.38 (d [br], J = 636.3, 9F, $^{-}OSO_2C\mathbf{F_3}$). HRMS calculated for $C_{28}H_{28}N_6F_6YbO_6S_2^+$ ([M - ($^{-}OSO_2CF_3$)]$^+$): calculated 896.0799, found 896.0804.

Synthesis of [Nd(ONO)tpen](OTf) complex

To a 20 mL scintillation vial, 159 mg (0.1566 mmol, 1.001 eq) of [Nd(tpen)(OTf)$_3$] was added and suspended in 4 mL of THF with stirring. Then, 46 mg (0.1565 mmol, 1 eq) of ONO was dissolved in 4 mL of THF and deprotonated with 11 mg (0.4583 mmol, 2.93 eq) of sodium hydride. Upon deprotonation, bubbles were observed, and the solution changed from clear to bright yellow green. The deprotonated ligand was filtered through a pipet into the salt

suspension to give an almost immediate color change to green. The solution was stirred overnight to ensure completion of reaction. The solvent was then removed in vacuo, and the remaining solid was washed with pentane and freeze dried in benzene to yield 141 mg (89.2%) of a green powder. Single crystals were grown by dissolving 50-75 mg of compound in 1,2-dimethoxyethane (DME) followed by slow diffusion of diethyl ether. Crystals formed overnight. ^{1}H NMR (CD_3CN, 400 MHz) δ (ppm): -11.13, -7.00, -4.91, -4.29, -2.52, 1.11, 1.61, 1.83, 2.51, 3.00, 3.46, 3.67, 6.09, 6.52, 7.19, 7.71, 8.44, 8.95, 9.65, 10.15, 10.49, 11.76, 12.74, 14.30, 14.58, 16.21, 17.06, 18.56, 19.69, 20.06, 23.37, 25.65, 25.98, 29.55, 32.05, 40.80. The NMR is broad due to fluxionality of ligand in solution showing the average of the species with differing ligand positions. As a result, accurate integrations for the spectra cannot be provided. All efforts to obtain ^{13}C NMR were unsuccessful due to paramagnetism in the compound. ^{19}F NMR (CD_3CN, 376.5 MHz) δ ppm: -79.33. HRMS calculated for $C_{44}H_{46}N_8NdO_2^+$ ([M - ($^-OSO_2CF_3$)]$^+$): 860.2815, found 860.2515. Elem. Anal. for $C_{45}H_{46}N_8F_3NdO_5S$ calc.: C, 53.40; H, 4.58; N, 11.07, found: C, 53.91; H, 4.88; N, 12.10.

Synthesis of [Er(ONO)tpen](OTf) complex

The same procedure as above was used in the preparation of the erbium complex to yield 86 mg (66.2%). ^{1}H NMR (DMSO-d_6, 400 MHz) δ ppm: -159.96, -131.20, -101.16, -91.92, -57.51, -49.04, -46.99, -33.12, -28.50, -24.90, -17.20, -14.73, 14.63, -10.84, -9.92, -9.45, -8.62, -7.31, -6.77, -6.57, 1.76, 3.61, 7.22, 7.41, 7.69, 8.44, 10.53, 15.40, 32.35, 34.94, 40.21, 41.34, 43.47, 44.83, 76.25, 84.47, 96.02. The NMR is broad due to fluxionality of ligand in solution showing the average of the species with differing ligand positions. As a result, accurate integrations for the spectra cannot be provided. All efforts to obtain ^{13}C NMR were unsuccessful due to paramagnetism in the compound. ^{19}F NMR (CD_3CN, 376.5 MHz) δ ppm: -79.32. HRMS calculated for $C_{44}H_{46}N_8ErO_2^+$ ([M - ($^-OSO_2CF_3$)]$^+$): 884.3041, found 884.2962. Elem. Anal. for $C_{45}H_{46}F_3N_8NdO_5S$ calc.: C, 52.21; H, 4.48; N, 10.82, found: C, 51.56; H, 4.21; N, 10.31.

Synthesis of [Yb(ONO)tpen](OTf) complex

The same procedure as above was used in the preparation of the erbium complex to yield 106 mg (70.0%) yellow solid. ^{1}H NMR (CD_3CN, 400 MHz) δ ppm: -103.37, -91.53, -75.36, -71.61, -52.47, -49.51, -41.56, -40.87, -37.69, -19.72, -19.45, -16.82, -13.92, -13.22, -11.29, -9.08, -8.51, -8.40, -8.29, -5.55, -5.42, -0.64, 1.86, 2.71, 3.56, 3.71, 7.21, 7.23, 7.26. 7.72, 8.50, 11.51,

14.48, 24.46, 25.65, 26.52, 35.89, 39.71, 40.78, 41.52, 43.82, 46.55, 49.77, 65.96, 71.98, 75.77. The NMR is broad due to fluxionality of ligand in solution showing the average of the species with differing ligand positions. As a result, accurate integrations for the spectra cannot be provided. All efforts to obtain ^{13}C NMR were unsuccessful due to paramagnetism in the compound. ^{19}F NMR (CD_3CN, 376.5 MHz) δ ppm: 79.38 (s, 3F, $^{-}OSO_2C\mathbf{F_3}$). HRMS calculated for $C_{44}H_{46}N_8YbO_2^+$ ([M - ($^{-}OSO_2CF_3$)]$^+$): 892.3147, found 892.3291. Elem. Anal. for $C_{45}H_{46}N_8F_3YbO_5S$ calc.: C, 51.92; H, 4.45; N, 10.76, found: C, 51.55; H, 4.11; N, 10.56.

NMR

Na_2ONO (L^{2-})

^1H (400.144 MHz, CD_3CN)

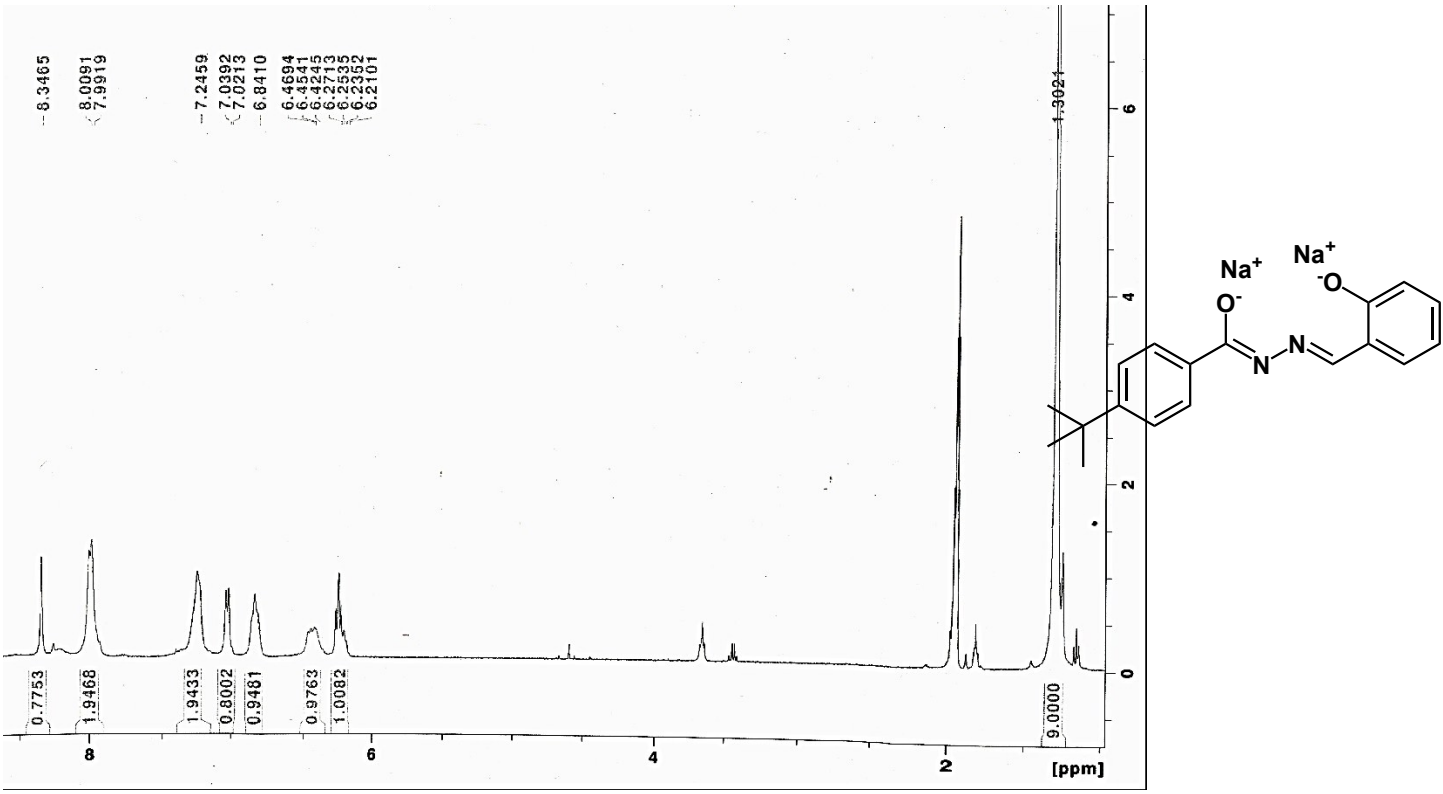

Figure S1: ^1H NMR of doubly deprotonated ligand in CD_3CN

[Nd(tpen)(OTf)$_3$]:

^{1}H (400.144 MHz, CD_3CN)

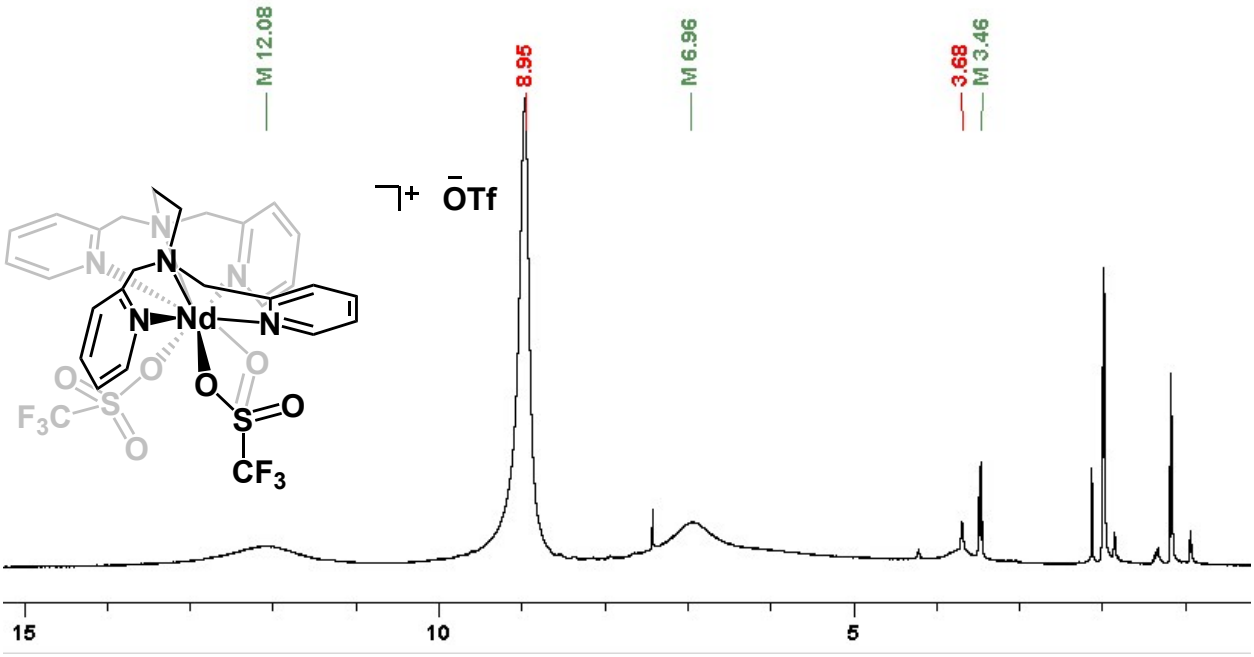

Figure S2: ^{1}H NMR of neodymium tpen complex in CD_3CN

^{19}F (376.512 MHz, CD_3CN)

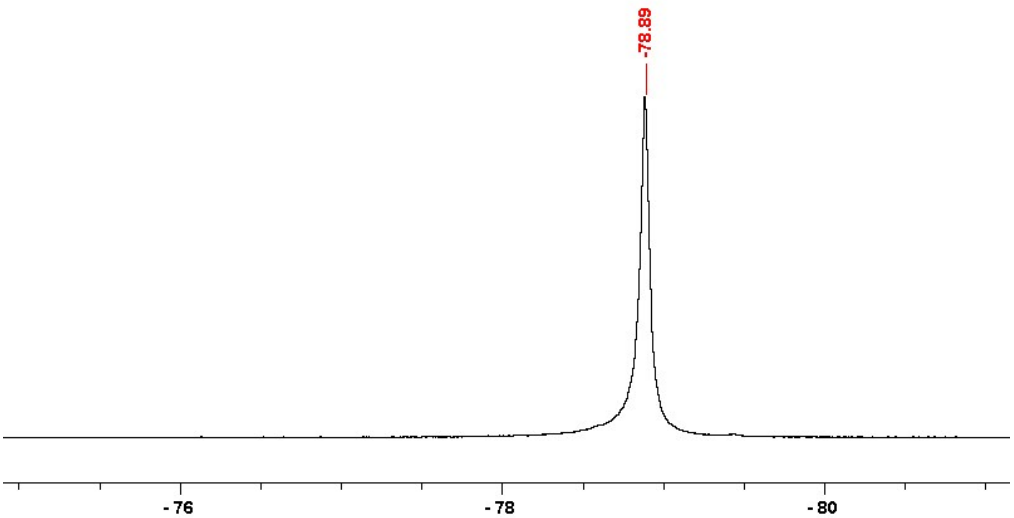

Figure S3: ^{19}F NMR of neodymium tpen complex in CD_3CN

[Er(tpen)(OTf)$_3$]:
^1H (400.144 MHz, CD_3CN)

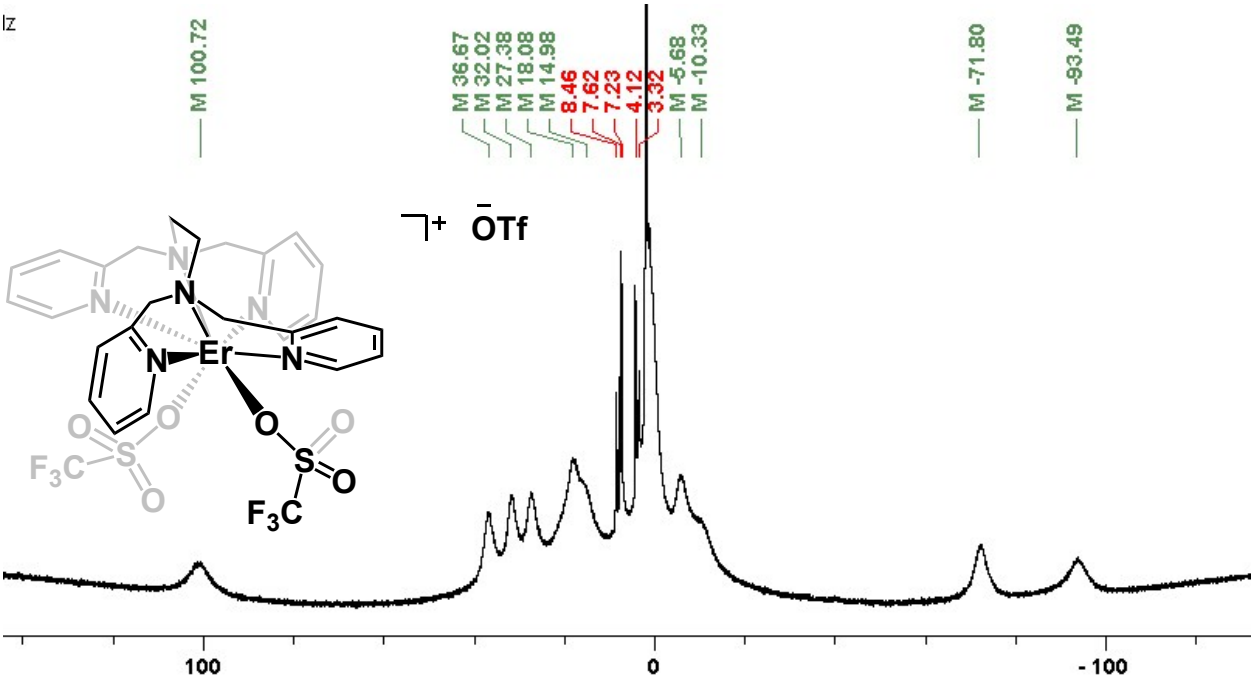

Figure S4: ^1H NMR of erbium tpen complex in CD_3CN

[Yb(tpen)(OTf)$_3$]:
^1H (400.144 MHz, CD_3CN)

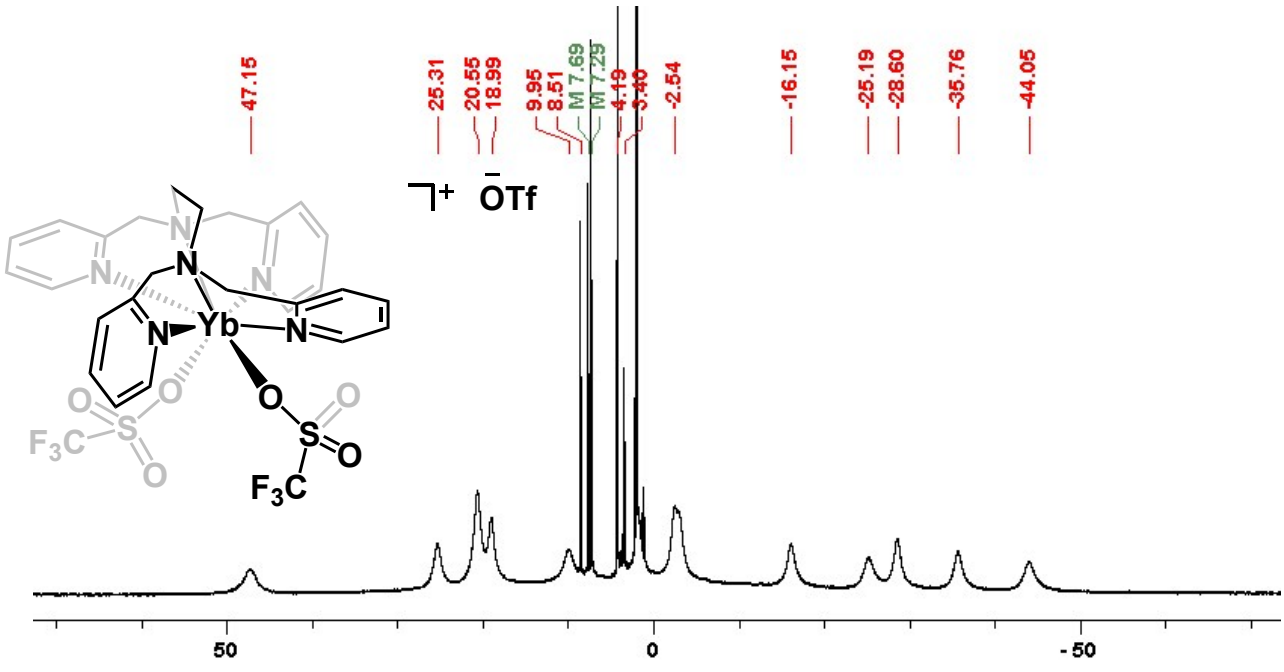

Figure S5: ^{1}H NMR of ytterbium tpen complex in CD_3CN
^{19}F (376.512 MHz, CD_3CN)

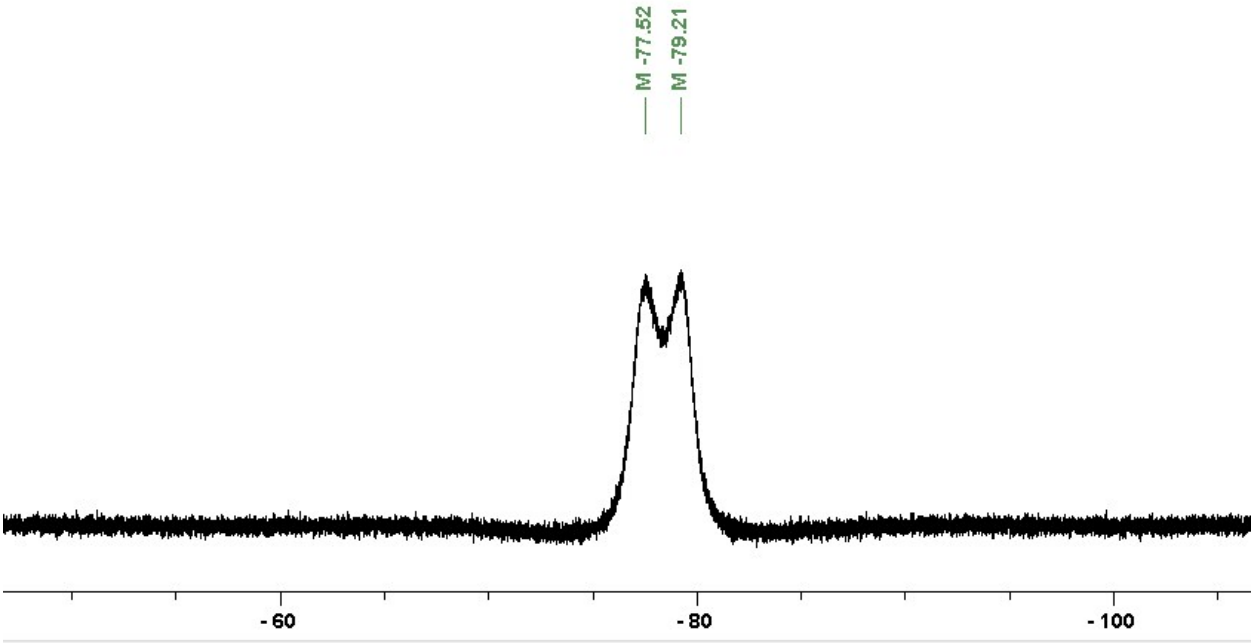

Figure S6: ^{19}F NMR of ytterbium tpen complex in CD_3CN

[Nd(ONO)tpen](OTf) complex
^{1}H (400.144 MHz, CD_3CN)

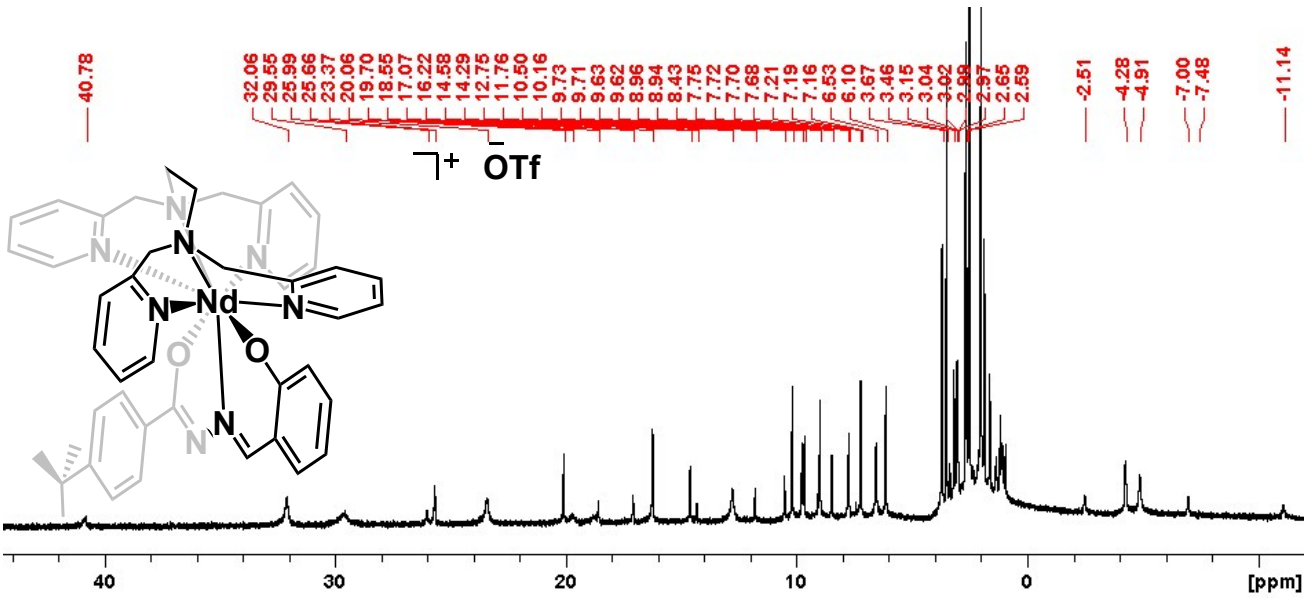

Figure S7: ^{1}H NMR of neodymium complex in CD_3CN

^{19}F (376.512 MHz, CD_3CN)

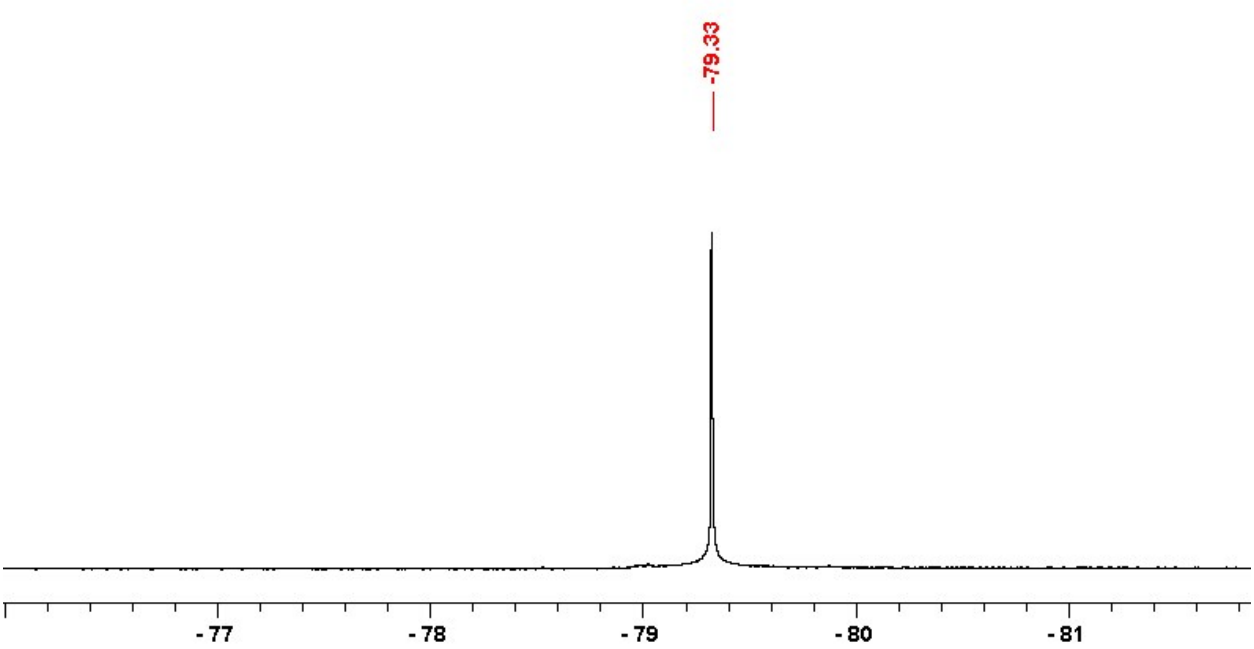

Figure S8: ^{19}F NMR of neodymium complex in CD_3CN

[Er(ONO)tpen](OTf) complex

^{1}H (400.144 MHz, CD_3CN)

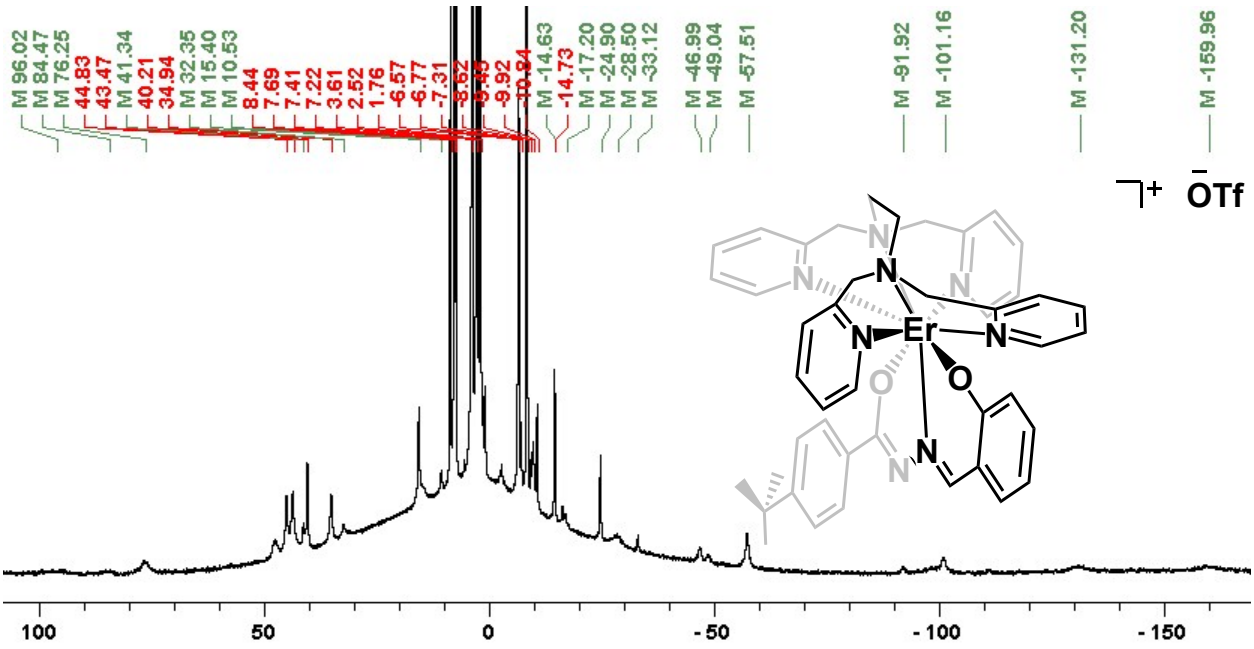

Figure S9: ^{1}H NMR of erbium complex in CD_3CN

^{19}F (376.512 MHz, CD_3CN)

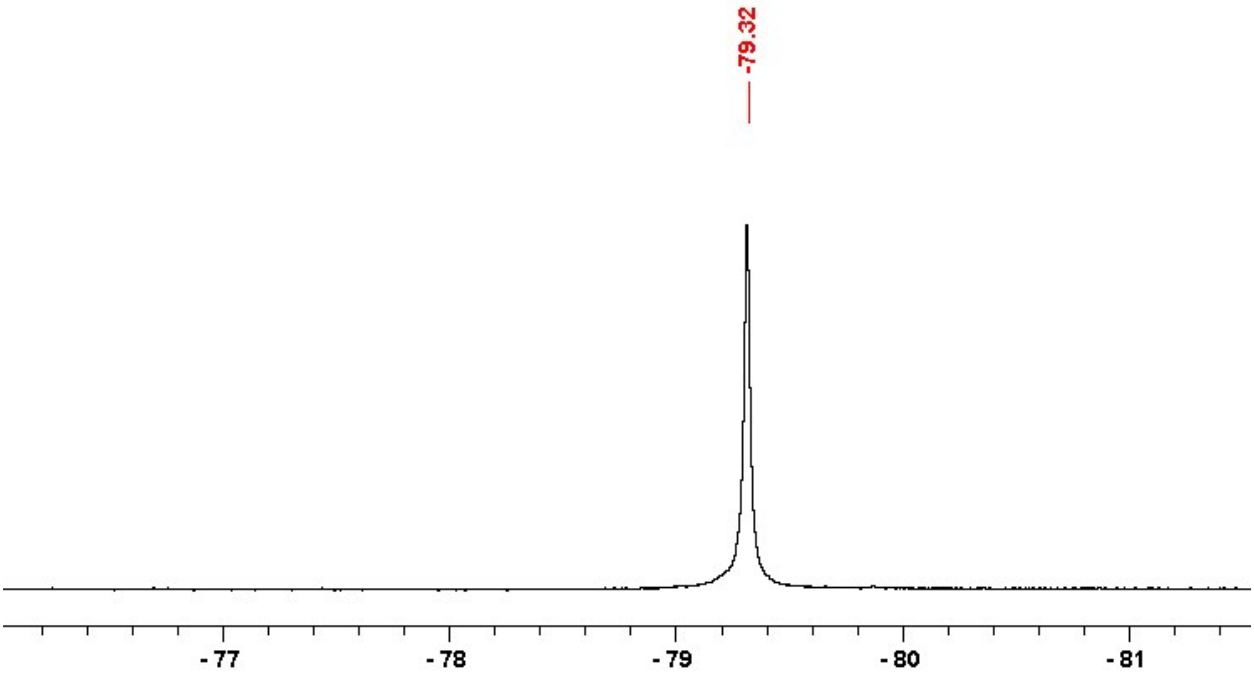

Figure S10: ^{19}F NMR of erbium complex in CD_3CN

[Yb(ONO)tpen](OTf) complex

^{1}H (400.144 MHz, CD_3CN)

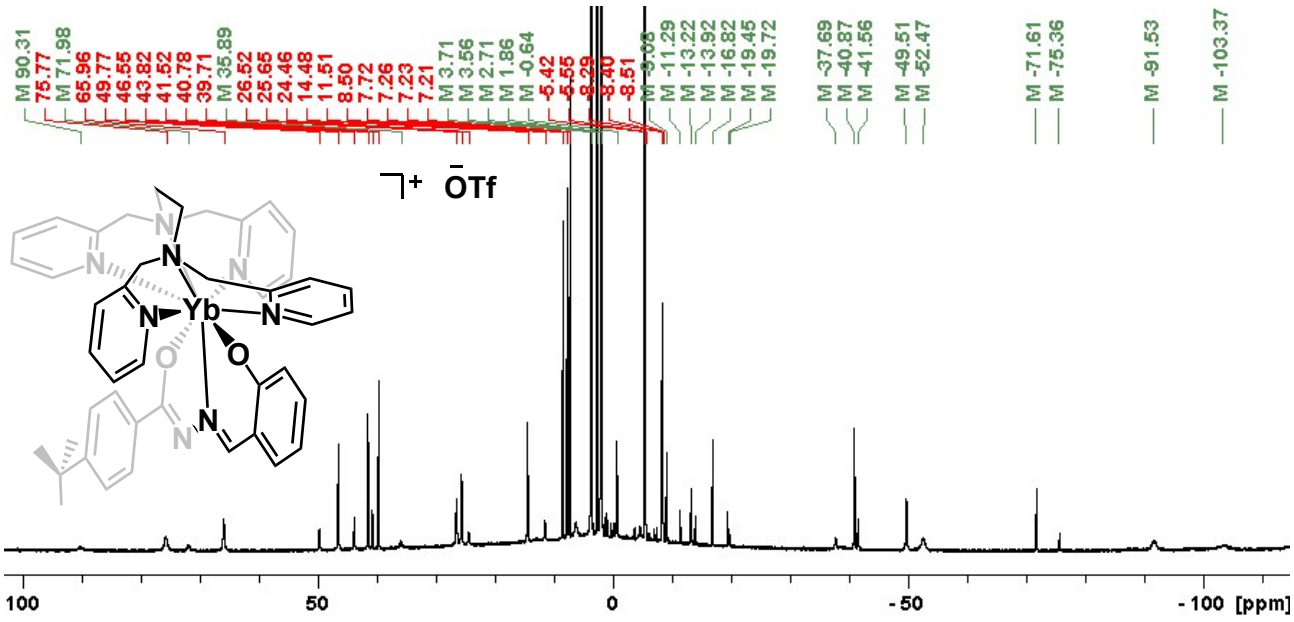

Figure S11: ^{1}H NMR of ytterbium complex in CD_3CN

^{19}F (376.512 MHz, CD_3CN)

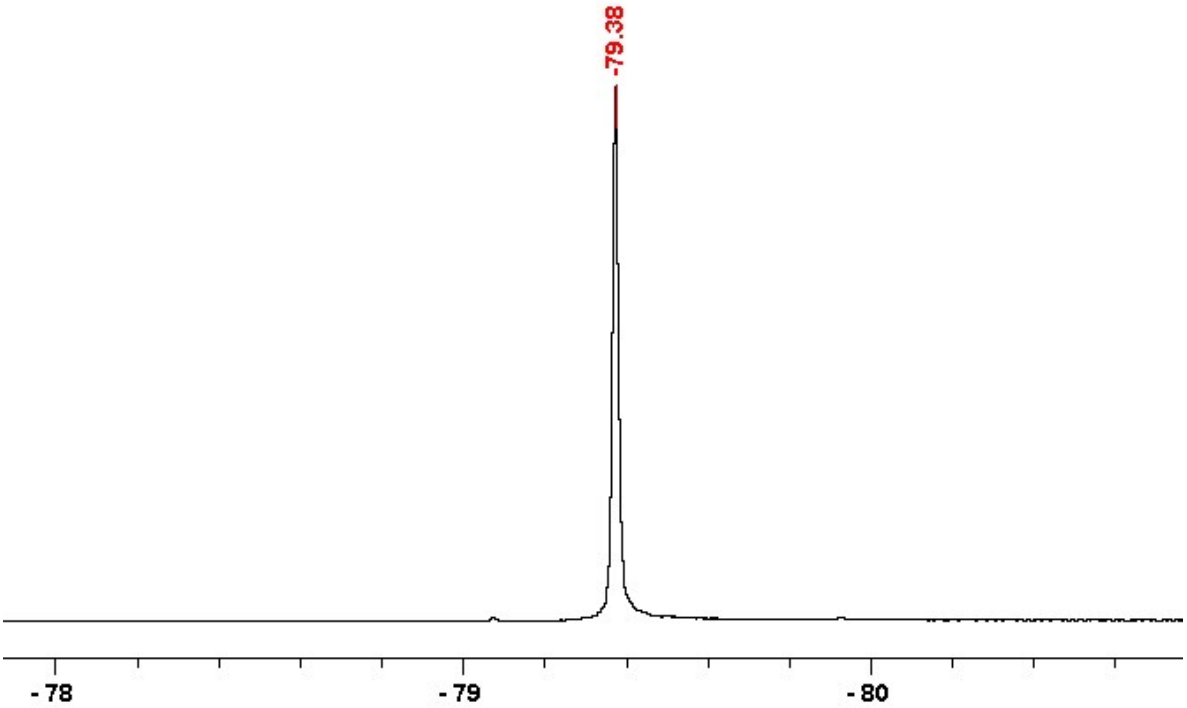

Figure S12: ^{19}F NMR of ytterbium complex in CD_3CN

[Nd(ONO)tpen](OTf) complex

^{1}H (500.13 MHz, CD_3CN)

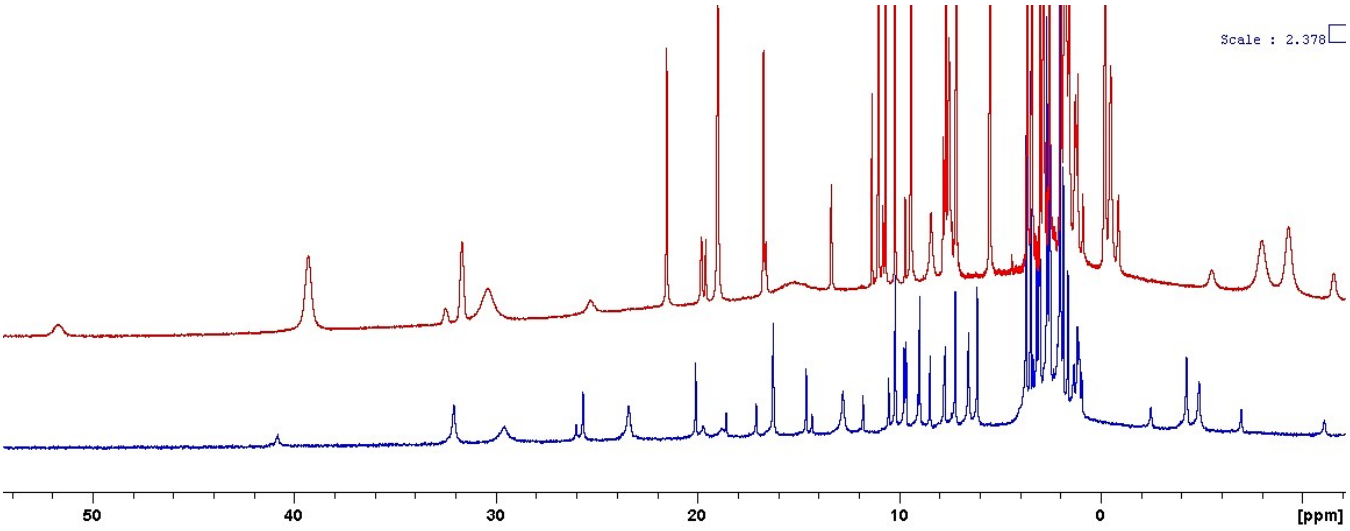

Figure S13: ^{1}H NMR of neodymium complex performed at 300K (blue) and 258K (red) to show as temperatures decrease, peaks have thermal shift and new peaks arise, indicating separate species.

High Resolution Mass Spectrometry

[Nd(ONO)tpen](OTf) complex

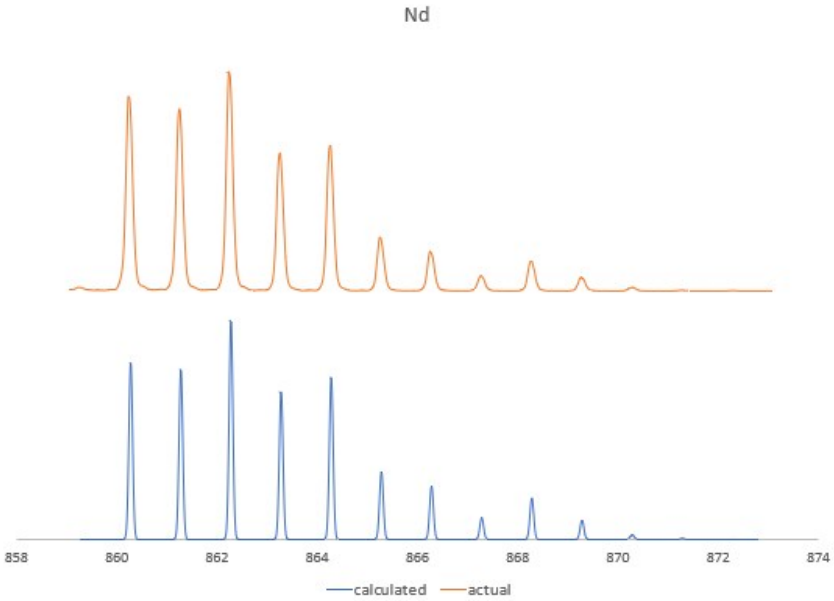

Figure S14: HRMS of neodymium complex versus calculated $C_{44}H_{46}N_8NdO_2^+$: 860.2515.

[Er(ONO)tpen](OTf) complex

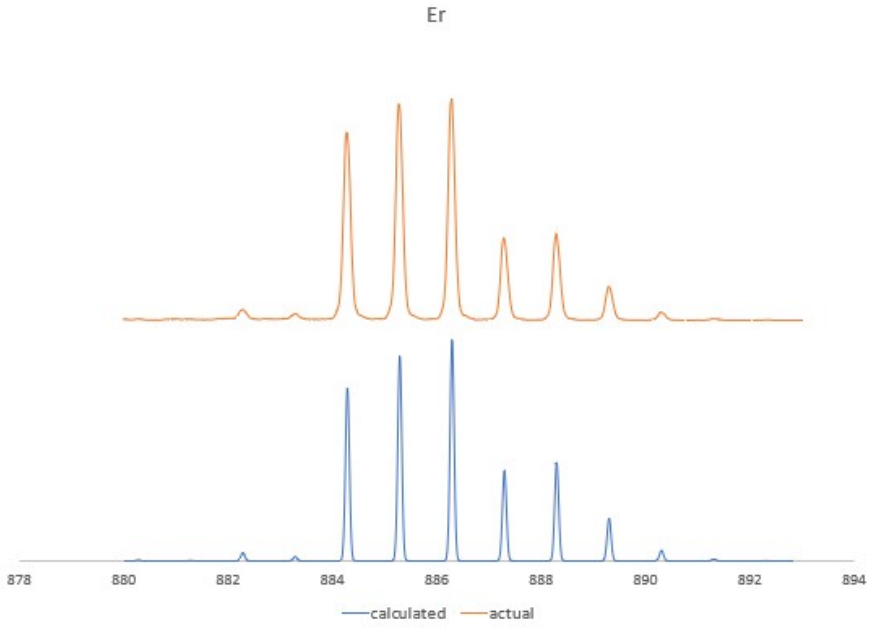

Figure S15: HRMS of erbium complex versus calculated $C_{44}H_{46}N_8ErO_2^+$: 884.2962.

[Yb(ONO)tpen](OTf) complex

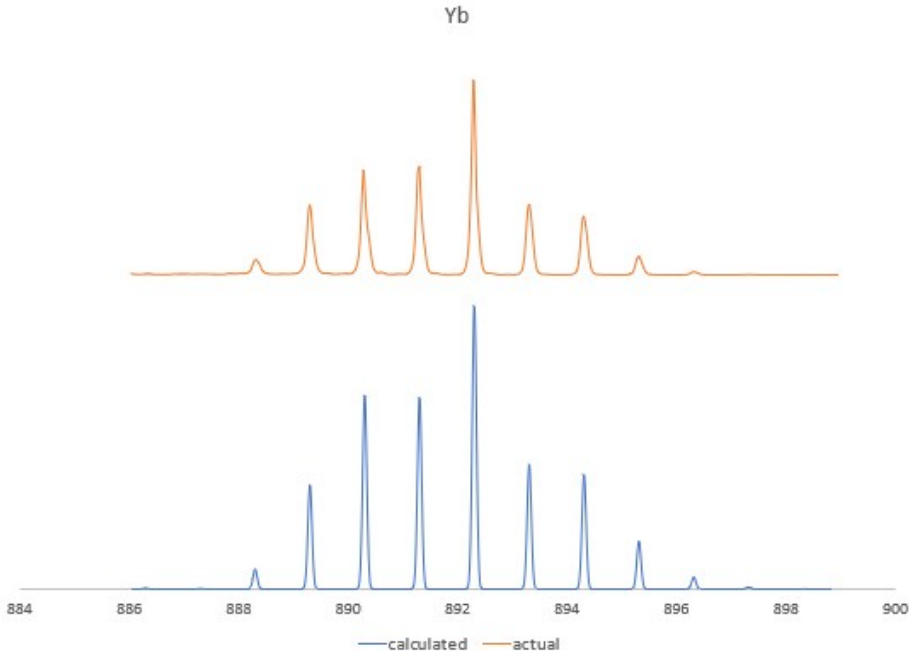

Figure S16: HRMS of ytterbium complex versus calculated $C_{44}H_{46}N_8YbO_2^+$: 892.3291.

Photophysical Data

Absorption and emission of LH_2 ligand

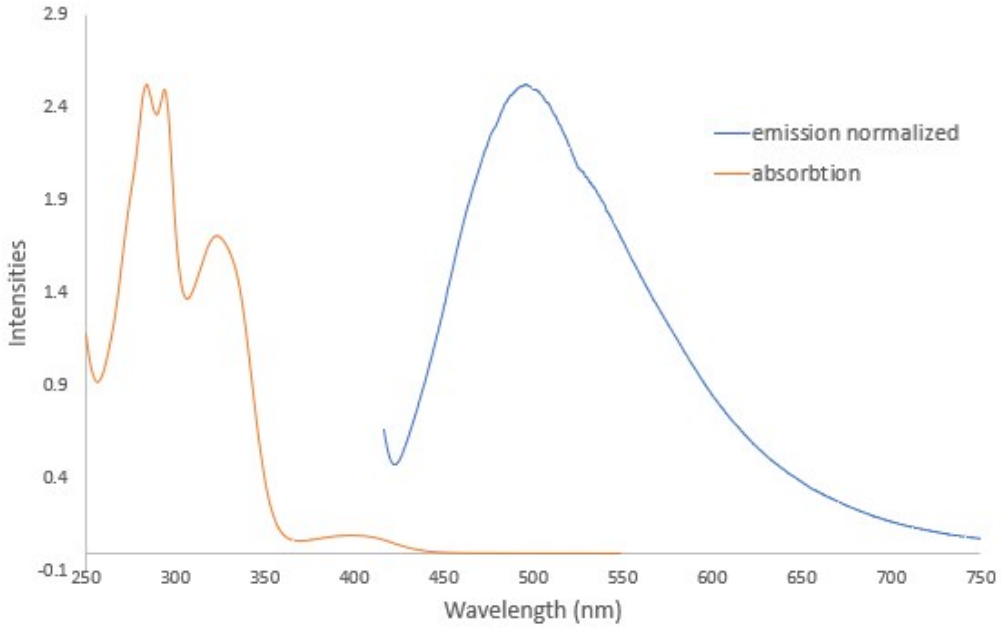

Figure S17: Absorption and emission of LH_2 ligand. 9.7 x 10^{-5} mol L^{-1} in CH_3CN. Excitation at 400 nm. Slit widths 20 nm.

Excitation, emission, and absorption of [Nd(ONO)tpen](OTf)

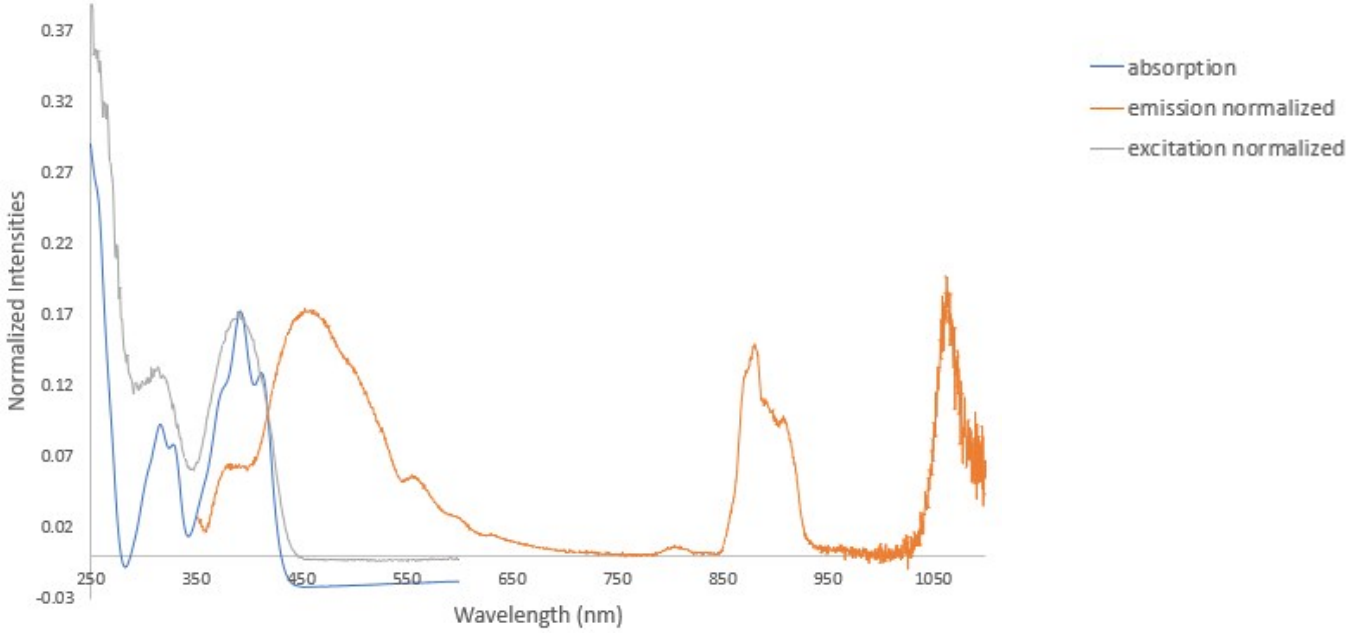

Figure S18: Absorption, excitation, and emission [Nd(tpen)(L)](OTf). 5.7 x 10^{-6} (abs, ex) and 7.4 x 10^{-7} mol L^{-1} (em) in CH_3CN. Excitation at 390 and 400 nm with slit widths 3.9 nm, 0.9 nm (ex/em) and 20 nm for emission and absorption/excitation respectively.

Excitation, emission, and absorption of [Yb(ONO)tpen](OTf)

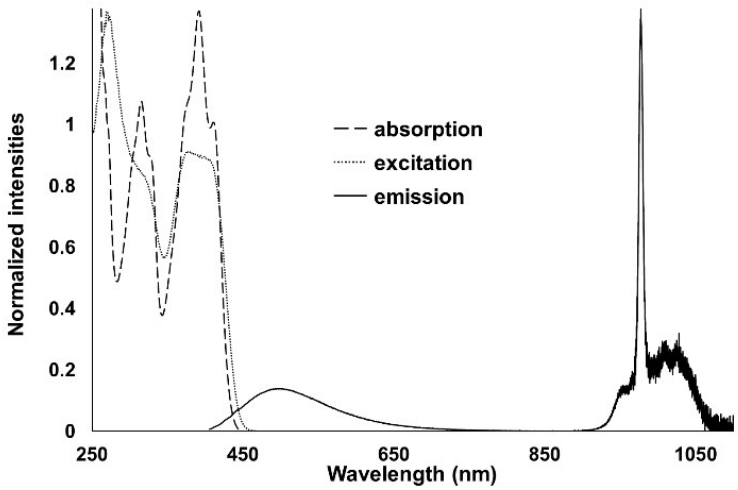

Figure S19: Absorption (dashed), excitation (dotted), and emission (solid) spectra of **[(Yb(ONO)tpen](OTf)** (9.7 x 10^{-6} mol L^{-1} in acetonitrile). Excitation collected for emission centred at 975 nm. Emission collected with excitation at 390 nm. Slit widths: 20 nm (excitation/emission).

Emission of [Yb(ONO)tpen](OTf) in 80:20 water to acetonitrile

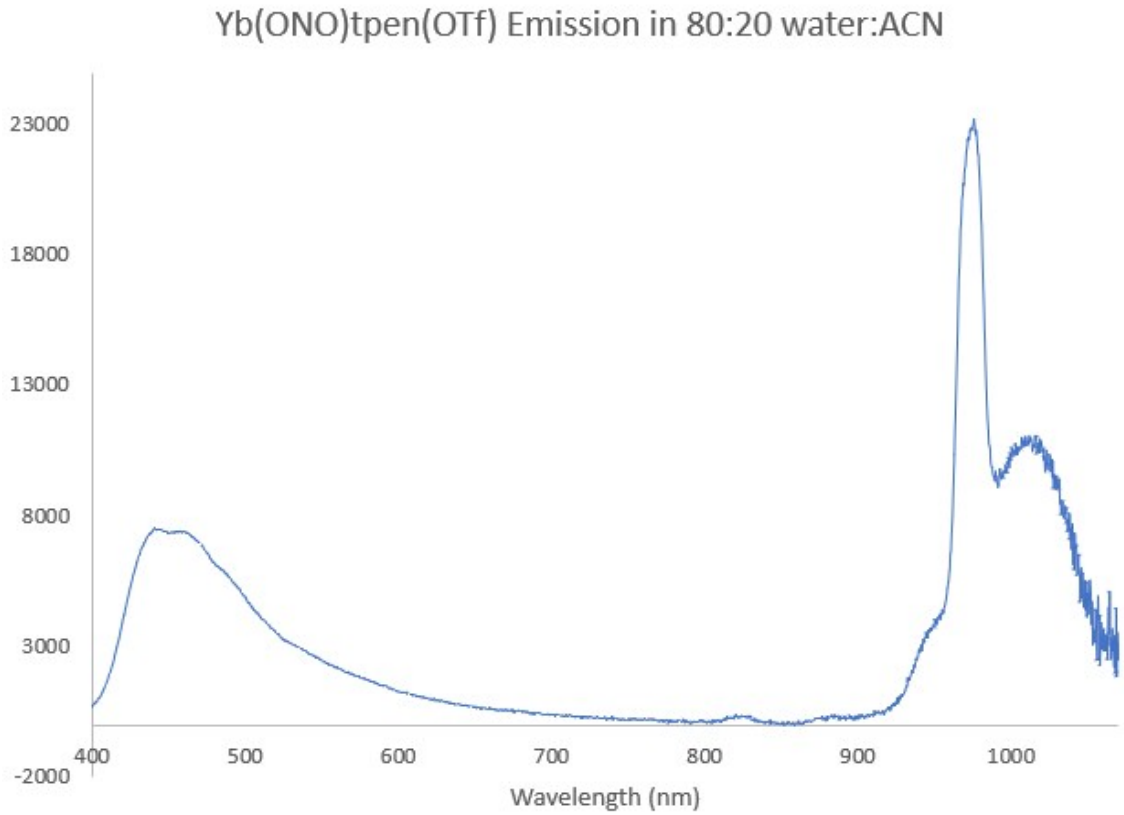

Figure S20: Emission of ytterbium complex in water abundant solution. Concentration > 9.6 x 10^{-5} mol L^{-1}. Excitation and emission slit widths 20 nm.

Quantum yield determination

Absolute quantum yields were determined by employing a barium sulfate coated integrating sphere using an Edinburgh FLS1000 fluorimeter. The integrating sphere was mounted on the fluorimeter with the entry and output ports of the sphere located in 90° geometry from each other in the plane of the spectrometer. The quantum yields were determined by measuring the visible peak as an internal standard. According to the integration ratio of the lanthanide peaks to the visible peak, the quantum yields of lanthanide emission were calculated from the absolute quantum yield of the visible emission.

The spectra were taken on an Edinburg fluorimeter equipped with two detectors, a PMT 980 for the visible region and an InGaAs for the NIR region. Since the detectors have different sensitivities, different layers of spectra were taken. The first being the visible region of the spectra down to about 950 nm. The next spectra taken was a smaller region using the PMT with a slower scan rate for better resolution, overlapping from about 850 to 970. After this, the detector was switched to the InGaAs and the first spectra taken was another overlap of the last, with a slow scan rate for good resolution from about 950 to 1100. Finally, the last spectrum was taken using the InGaAs overlapping from 1000 down as far as each metal needed into the infrared region. If any peak was poorly resolved, an additional spectrum was taken with overlapping pieces and slower scan rates to get a better resolution. After all spectra were acquired, each in turn using an overlapping wavelength was normalized to the one before it until all essentially were normalized to the first PMT spectrum.

Using the integrating sphere, the quantum yield for the visible was measured to be 2.11%, corresponding to a quantum yield in the near-infrared region of 16.1%.

Because of potential mis-normalization, we have measured the quantum yields using external standards according to the following equation:

$$\Phi_{Sam} = \Phi_{Std} \times \frac{kSam}{kStd} \times \left(\frac{\eta Sam}{\eta Std}\right)_2$$

Where Std and Sam denote standard and sample, respectively; Φ is the quantum yield; k is the slope from the plot of integrated emission intensity vs absorbance, and η is the refractive index of the solvent.

9,10-diphenylanthracene was utilized as standard in the visible region, and $Yb(TTA)_3(H_2O)_2$ was utilized in the near-infrared region. Quantum yields of 1.5% and 21% were measure for the visible and near-infrared regions, respectively. These results are in line with the results obtained from the absolute method described above. Because the estimated error of quantum yield measurement is typically 10-15%, we prefer disclosing the number obtained from the absolute method in the manuscript.

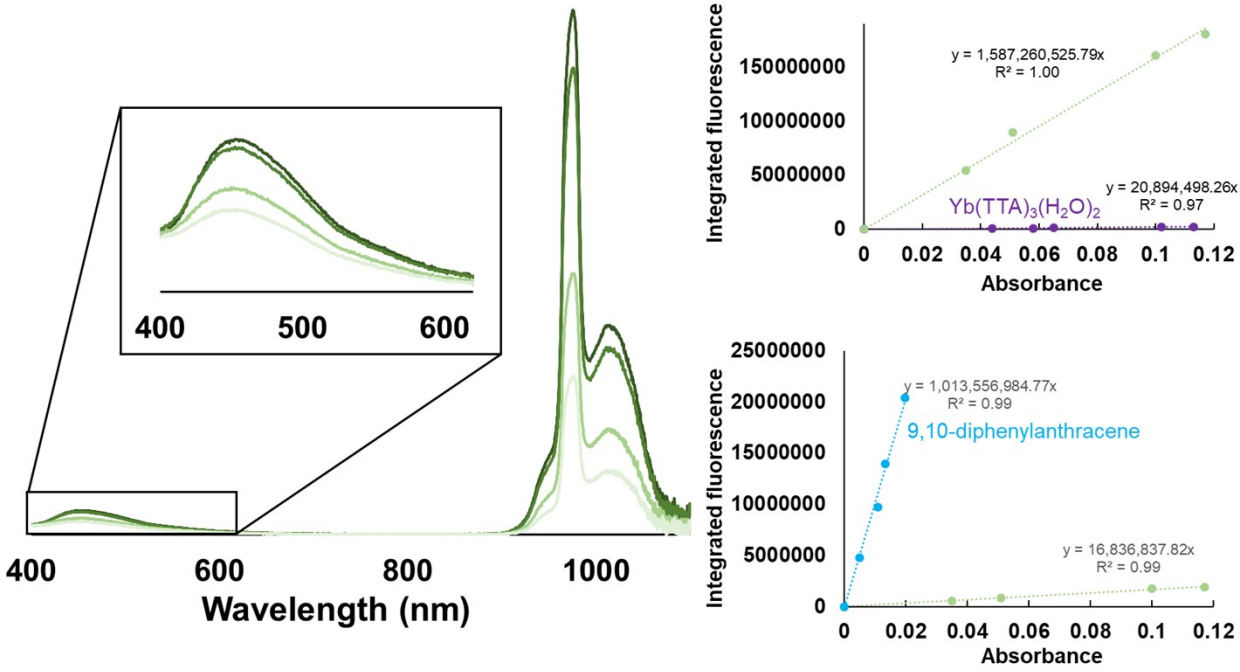

Figure S21: Emission at various absorbances, and plots of emission intensity vs absorbance.

Additionally, we performed an experiment synthesizing an $Yb(L)_2$ complex to have a closer system analog to those reported in literature. The quantum yield was measured using the absolute quantum yield method with the integrating sphere and found to be 2.37% in acetonitrile for the NIR region. This value is close to the reported value of 3.62% for the M_2L_2 structure reported by Han referenced in the main text.

X-Ray Crystallography

N_{tpen} – Ln bond distances

Table S1: Bond distances between tpen nitrogens and lanthanides in their respective complexes

	L		*en*				
	N1	N2	N3	N4	N5	N6	N7
Nd	2.556(4)	2.736(3)	2.676(4)	2.655(4)	2.720(4)	2.606(4)	2.694(4)
Er	2.491(3)	2.667(3)	2.598(3)	2.554(3)	2.672(3)	2.514(3)	2.625(3)
Yb	2.470(3)	2.582(2)	2.604(3)	2.502(3)	2.660(2)	2.541(3)	2.678(4)

Geometry comparison of precursors and products

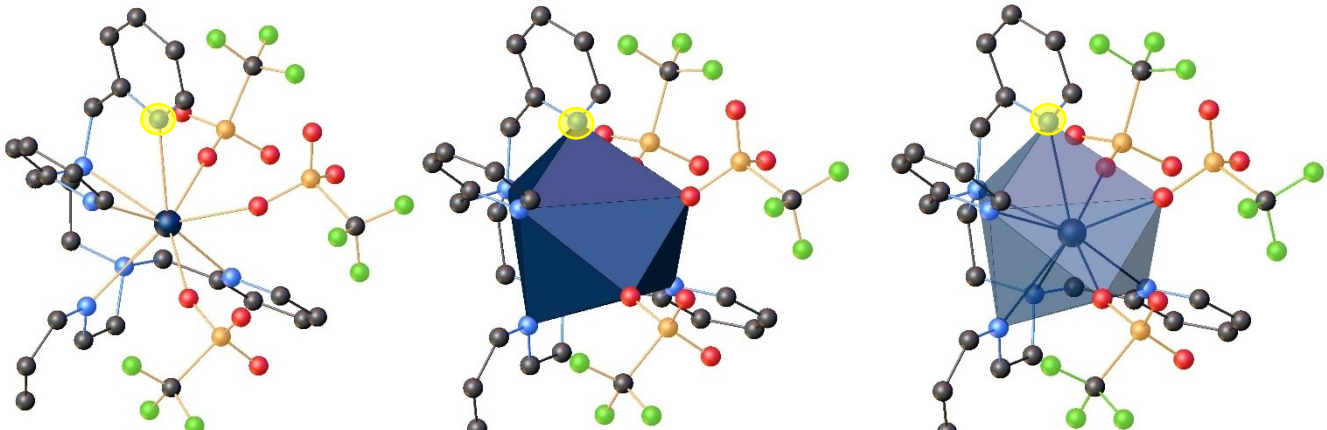

Figure S22: Comparison of metal geometry for [La(tpen)$(OTf)_3$] precursor (top) and [Ln(ONO)tpen](OTf) complexes (bottom). Where the "cap" [highlighted in yellow] in the capped square antiprism differs; and is a nitrogen from a pyridine and the nitrogen from the salicylhydrazone ligand for the precursors and products respectfully.

[Nd(ONO)tpen](OTf) complex

Table S2: Crystal data and structure refinement for KMA311_ndmono.

Identification code	KMA311_ndmono
Empirical formula	$C_{47}H_{46}F_3N_8NdO_{5.5}S$
Formula weight	1044.22
Temperature/K	100.01(10)
Crystal system	monoclinic
Space group	I2/a
a/Å	37.8547(6)
b/Å	9.37739(14)
c/Å	26.6795(4)
α/°	90
β/°	97.8320(15)
γ/°	90
Volume/Å^3	9382.3(3)
Z	8

ρ_{calc}g/cm^3	1.478
μ/mm^{-1}	9.428
F(000)	4248.0
Crystal size/mm^3	0.202 × 0.081 × 0.01
Radiation	CuKα (λ = 1.54184)
2Θ range for data collection/°	6.688 to 147.448
Index ranges	-46 ≤ h ≤ 47, -8 ≤ k ≤ 11, -28 ≤ l ≤ 33
Reflections collected	35768
Independent reflections	9266 [R_{int} = 0.0457, R_{sigma} = 0.0543]
Data/restraints/parameters	9266/121/645
Goodness-of-fit on F^2	1.029
Final R indexes [I>=2σ (I)]	R_1 = 0.0440, wR_2 = 0.1148
Final R indexes [all data]	R_1 = 0.0552, wR_2 = 0.1233
Largest diff. peak/hole / e Å^{-3}	1.36/-0.65

[Er(ONO)tpen](OTf) complex

Table S3: Crystal data and structure refinement for KMA259_ermono.

Identification code	KMA259_ermono
Empirical formula	$C_{47}H_{51}ErF_3N_8O_6S$
Formula weight	1080.28
Temperature/K	100.00(10)
Crystal system	monoclinic
Space group	I2/a
a/Å	26.8628(4)
b/Å	9.29634(17)
c/Å	37.5992(5)
α/°	90
β/°	98.6743(13)
γ/°	90
Volume/Å^3	9282.1(3)
Z	8
ρ_{calc}g/cm^3	1.546
μ/mm^{-1}	1.923
F(000)	4384.0

Crystal size/mm^3	0.285 × 0.097 × 0.023
Radiation	MoKα (λ = 0.71073)
2Θ range for data collection/°	4.03 to 51.362
Index ranges	-32 ≤ h ≤ 32, -11 ≤ k ≤ 11, -45 ≤ l ≤ 45
Reflections collected	39160
Independent reflections	8832 [R_{int} = 0.0506, R_{sigma} = 0.0439]
Data/restraints/parameters	8832/0/599
Goodness-of-fit on F^2	1.066
Final R indexes [I>=2σ (I)]	R_1 = 0.0357, wR_2 = 0.0690
Final R indexes [all data]	R_1 = 0.0445, wR_2 = 0.0722
Largest diff. peak/hole / e Å^{-3}	1.56/-0.79

[Yb(ONO)tpen](OTf) complex

Table S4: Crystal data and structure refinement for KMA363_ybmono.

Identification code	KMA363_ybmono
Empirical formula	$C_{47}H_{51}F_3N_8O_6SYb$
Formula weight	1086.06
Temperature/K	100.01(10)
Crystal system	monoclinic
Space group	C2/c
a/Å	49.2884(8)
b/Å	9.28670(10)
c/Å	26.8502(4)
α/°	90
β/°	131.202(3)
γ/°	90
Volume/Å^3	9246.9(4)
Z	8
ρ_{calc}g/cm^3	1.560
μ/mm^{-1}	4.752
F(000)	4400.0
Crystal size/mm^3	0.169 × 0.069 × 0.046
Radiation	CuKα (λ = 1.54184)
2Θ range for data collection/°	6.66 to 147.18

Index ranges	$-54 \leq h \leq 60$, $-11 \leq k \leq 11$, $-33 \leq l \leq 33$
Reflections collected	85837
Independent reflections	9275 [R_{int} = 0.0258, R_{sigma} = 0.0110]
Data/restraints/parameters	9275/0/599
Goodness-of-fit on F^2	1.045
Final R indexes [I>=2σ (I)]	R_1 = 0.0336, wR_2 = 0.0845
Final R indexes [all data]	R_1 = 0.0341, wR_2 = 0.0848
Largest diff. peak/hole / e $Å^{-3}$	2.57/-1.29

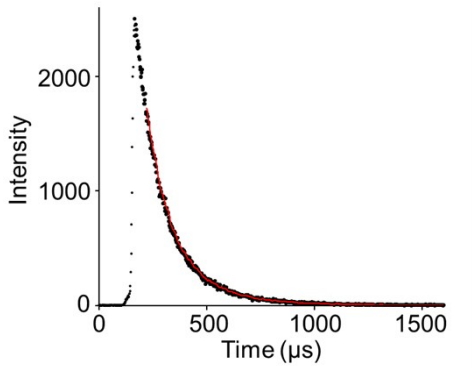

Figure S23. Luminescence decay profile of the transition $^2F_{5/2} \rightarrow {}^2F_{7/2}$ for **[(tpen)Yb(L)][OTf]** in CH_3CN

Fit of the luminescence decay profile yielded an observed lifetime τ_{obs} = 165 µs.

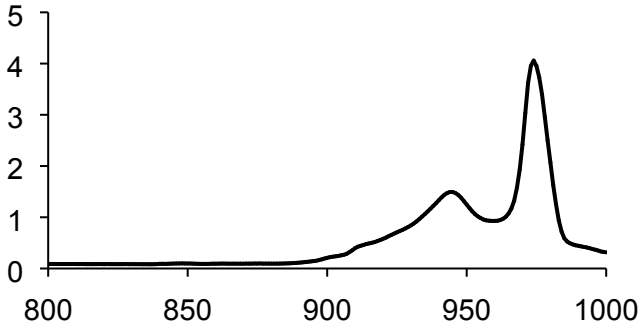

Figure S24. Absorption spectrum of **[(tpen)Yb(L)][OTf]** in CH_3CN in the near-infrared region.

The *f-f* absorption spectrum allows us to estimate the radiative lifetime τ_{rad} based on a modified Einstein equation.[6]

$$\frac{1}{\tau rad} = 2303 \times \frac{8\pi c \upsilon^2 n^2 (2J+1)}{NA(2J^{'}+1)} \times \int \varepsilon(\upsilon) d(\upsilon)$$

where c is the speed of light, n is the refractive index, υ is the barycenter of the transition, N_A is Avogadro's number, J and J' are the quantum numbers for the ground and excited states, espectively, and the integral is the integrated spectrum of the transition,

The τ_{rad} was calculated to be 0.70 ms.

These lifetimes indicate a sensitization efficiency η of 68% for our ligands, according to the following equation.[6]

$$\Phi = \eta \times \frac{\tau obs}{\tau rad}$$

References

1. Edward et al. *J. Chem. Eng. Data*. **1988**, *33(4)*, 538-540.
2. (a) Johnson et al. *J. Am. Chem. Soc.* **2013**, *135(47)*, 17723. (b) Sato et al. *Synthesis*, **1992**, *6*, 539.
3. Dolomanov, O. V.; Bourhis, L. J.; Gildea, R. J.; Howard, J. A. K.; Puschmann, H. *J. Appl. Crystallogr*. **2009**, *42*, 339.
4. Sheldrick, G. M. *Acta Crystallogr., Sect. A: Found. Crystallogr.* **2008**, *64*, 112.
5. Natrajan et al. *Dalton Trans*. **2006**, *8*, 1002.
6. a) J. Hu, Y. Ning, Y. Meng, J. Zhang, Z. Wu, S. Gao, and J. Zhang. *Chem. Sci*., **2017**, *8*, 2702-2709. b) M. H. V. Werts, R. T. F. Jukes and J. W. Verhoeven, *Phys. Chem. Chem. Phys.*, **2002**, *4*, 1542–1548